ISSN 1070-4272, Russian Journal of Applied Chemistry, 2009, Vol. 82, No. 7, pp. 1211−1221. © Pleiades Publishing, Ltd., 2009.
Original Russian Text © B.F. Minaev, V.A. Minaeva, G.V. Baryshnikov, M.A. Girtu, H. Agren, 2009, published in Zhurnal Prikladnoi Khimii, 2009, Vol. 82, No. 7, pp. 1115−1125.

PHYSICOCHEMICAL STUDIES OF SYSTEMS AND PROCESSES

Theoretical Study of Vibration Spectra of Sensitizing Dyes for Photoelectrical Converters Based on Ruthenium(II) and Iridium(III) Complexes

B. F. Minaev[a], V. A. Minaeva[a], G. V. Baryshnikov[a], M. A. Girtu[b], and H. Agren[c]

[a]*Khmel'nitskii National University, Cherkassy, Ukraine*
[b]*Ovidius University of Constanta, Romania*
[c]*Royal Technological Institute, Stockholm, Sweden*

Received March 10, 2009

Abstract—Quantum-chemical method of the density functional theory was employed to calculate, with the use of a B3LYP hybrid exchange-correlation functional, the IR absorption and Raman spectra of $[Ru(bpy)_2(CN)_2]$ and $[Ir(bpy)_2(CN)_2]^+$ complexes. All the normal vibrational frequencies were analyzed and new assignments of a number of bands in the IR absorption and Raman spectra were made. The role of vibrational motions of metal atoms and ligands in the vibronic deformation of electron shells in the course of electron transfer was discussed. This was done using data on surface-enhanced Raman spectra of $[Fe(bpy)_2(CN)_2]$ and $[Ru(bpy)_3]^{2+}$ complexes adsorbed on the surface of colloid silver.

DOI: 10.1134/S1070427209070106

Dye-sensitized solar cells (DSSC) based on TiO_2 crystals are of considerable interest as renewable power sources because of providing a high coefficient of light conversion to electricity (up to 10.4%) [1–3]. DSSCs commonly use sensitizers based on complexes of ruthenium with bipyridine (bpy) and other organic ligands [1–4]. The most successful example of DSSC is a Gratzel cell in which ruthenium(II) bis(4,4'-dicarboxy-2,2'-bipyridyl)-bis(isothiocyanate) is used as sensitizer; similar dyes with cyano ligands [1–3] and without carboxy groups also served for this purpose. All these organometallic dyes absorb visible light and, being in the excited state, provide electron transfer to TiO_2 crystals on whose surface they are adsorbed. After that, the oxidized chromophore is reduced by the electrolyte and the cycle is repeated.

The requirements to a sensitizing chromophore are universal: high light absorption coefficient in the entire intense solar spectrum, ability to inject an electron into the conduction band of TiO_2, and fast reduction by the electrolyte. The choice and optimization of the chromophore are highly important for the DSSC technology. To make such a systematic choice, it is necessary to know the relationship between the structure and optical properties of dye molecules. For this purpose, a number of quantum-chemical calculations of electron absorption spectra of the most important sensitizers based on complexes of ruthenium(II) and iridium(III) with polypyridines have been carried out in recent years [2–5]. However, their IR and Raman spectra have not been calculated using modern methods of quantum chemistry with full configuration optimization; in [6, 7], vibration spectra of comparatively small fragments of complex ions were calculated.

Calculations based on the density functional theory (DFT) seem to be necessary for the following reasons. Primarily, the configuration optimization of bipyridyl complexes of ruthenium(II) and iridium(III), based on a search for the minimum of the full energy gradient "E/"q_i, and a simultaneous calculation of force constants, i.e., second derivatives "^2E/"q_i^2 with respect to all internal coordinates q_i, are related tasks. Their solution makes it possible to establish a profound relationship between the structure and the observed IR and Raman spectra, which

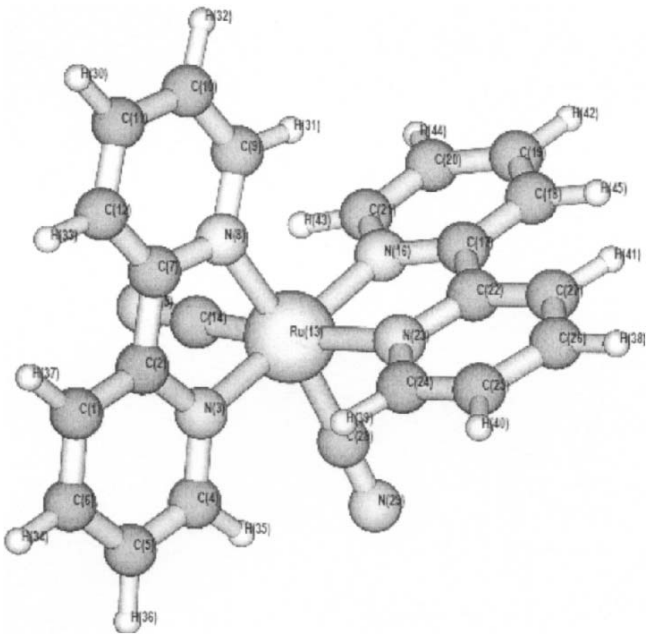

Fig. 1. Optimized structure and atom numbering for the $[Ru(bpy)_2(CN)_2]$ complex.

can be used to develop criteria for choice of sensitizers for DSSC, together with determining a correlation between the structure and electronic absorption and luminescence spectra. These latter are also important for designing organic light-emitting diodes (OLEDs). Although the functions of dyes in DSSC and OLED devices are the opposite, the common theoretical approach to both types of dye molecules seems to be useful.

The success in choosing and synthesizing efficient light emitters in OLEDs and dyes-converters of luminous energy to electricity in DSSCs depends on the knowledge of the nature of excited states of these molecules and their capacity for electron transfer. As follows from calculations, molecules of the $[Ru(bpy)_2(CN)_2]$ and $[Ir(bpy)_2(CN)_2]^+$ types are closely similar in structure, as well as in IR and Raman spectra. A certain analogy is observed in electronic absorption spectra of these sensitizing dyes in the UV and visible spectral ranges. To reveal a deeper correlation between their capacity for electron transfer and luminescence, a detailed knowledge of all the vibration modes and their activity in IR, Raman, and vibronic optical absorption and luminescence spectra is required. It is these effects of electron-vibration (vibronic) interaction and Frank–Condon factors that determine the rates of energy and electron transfer and those of intercombination and internal conversion [3], which is of fundamental importance for selection of dyes for DSSCs and OLEDs.

Electron transfer from an excited dye molecule must be induced by an electron–electron interaction between the surface of the semiconductor and an electron shell of the dye, with the vibrational motion of nuclei presumably being the driving force for the electron transfer, because only this motion governs the dynamics of all kinetic processes. It is the vibronic perturbation by intermolecular modes mixed with internal vibrations of the dye that induces the electron transfer and generates a current in the DSSC circuit.

In adsorption of ruthenium complexes on the surface of nanoclusters of silver and other metals, the so-called surface-enhanced resonance Raman scattering (SERRS) is observed. To determine the nature of the SERRS effect and its relation to the electron transfer and operation efficiency of solar cells, it is necessary to know in detail the vibrational frequencies of the organometallic complexes themselves, used in DSSC. As model sensitizers for DSSCs and OLEDs were chosen the simplest complexes of ruthenium(II) and iridium(III) with bipyridyl and cyano ligands, which have already been studied experimentally and exhibit basic features of most of other dyes. These are compounds $[Ru(bpy)_2(CN)_2]$ and $[Ir(bpy)_2(CN)_2]^+$, further designated as complexes (I) and (II). In this study, a detailed analysis of IR and Raman spectra of these dyes and of the relationship between the spectra and their structure was made using a modern, sufficiently precise, quantum-chemical method.

Calculation procedure. The equilibrium configurations, IR spectra, and Raman spectra of complexes (I) and (II) were calculated in terms of the density functional theory (DFT) by the B3LYP method (Becke–Lee–Yang–Parr three-parameter hybrid exchange-correlation functional) in the Lan12DZ basis set of atomic orbitals by the GAUSSIAN 03 software package [11]. The vibrational frequencies were calculated by analytical calculations of Hessian matrix for the equilibrium configuration, optimized in the ground (singlet) state.

The calculated forms of normal vibrations were compared with the published band assignment in Raman spectra of the complexes $[Ru(bpy)_2(phen)]^{2+}$ (phen is 1,10-phenanthroline [12]), $[Ru(bpy)_2(BIK)]^{2+}$ {BIK is a bidentate ketone [bis(1-methylimidazol-2-yl) ketone [13]}, $[Fe(bpy)_2(CN)_2]$, and $[Ru(bpy)_3]^{2+}$ [14] and with characteristic IR group frequencies [15]. This comparison made it possible to assess the potential of this calculation procedure for prediction of frequencies and forms of vibrations and absorption band intensities in IR and

Raman spectra of the complexes under study, to estimate the correction for the vibrational anharmonicity and electron correlation (scaling factor), and to assign those bands in the experimental spectra of Ru(II) complexes [12–14], whose vibration forms had not been described in the literature. The averaged value of the scaling factor for the vibrational frequencies was 0.9756.

Structural analysis of $[Ru(bpy)_2(CN)_2]$ and $[Ir(bpy)_2(CN)_2]^+$ complexes. The numbering of atoms and the optimized configuration of the $[Ru(bpy)_2(CN)_2]$ complex are shown in Fig. 1, and some of the calculated equilibrium configuration parameters of complexes (I) and (II) are listed in Table 1. As can be seen in Table 1, the calculation procedure overestimates the bond lengths between the metal ion and ligands (by 0.03 Å, on average). It is noteworthy that the lengths of these bonds are shorter for the Ir(III) complex, compared with the Ru(II) complex, which must reflect on the corresponding frequencies in the vibration spectra. This particularly refers to the bond with CN ligands. The presence of these ligands also leads to nonequivalence of the M–N bonds for bipyridyl ligands: the asymmetry of the $M–N_3$ and $M–N_8$ bond lengths reaches a large value (~0.05 Å), in agreement with X-ray diffraction data [16]. At the same time, the structural differences between the bpy ligands in both complexes are small (d”0.005E), i.e., the nature of the metal ion has nearly no effect on the configuration of the bipyridyl ligands.

When complexes (I) and (II) are formed, the C–C bridge bond becomes shorter (by 0.02 Å on average), as also does the C=C bond of pyridine rings, and the lengths of bonds adjacent to the nitrogen atom, via which the ligand is coordinated with the Ru(II) or Ir(III) ion, increase. In a calculation of the free ligand 2,2'-bipyridyl in the *cis* conformation, the most stable form is the conformer having a C_2 symmetry, with a dihedral angle between the rings equal to 43°. In the complexes under study, the *cis* conformation of 2,2’-bipyridyl takes a nearly planar structure: the dihedral angle between the rings is smaller than 1° (Table 1).

The difference between the energies of molecular orbitals (MO) of both complexes, $[M(bpy)_2(CN)_2]_n^+$, is large, which is accounted for by the difference between the charges of the complexes [$n = 0$ for complex (I) and $n = 1$ for complex (II)]. The large positive charge of the Ir(III) ion leads to a substantial decrease in the energies of the highest occupied (HO) and lowest unoccupied (LU) molecular orbitals (–0.345 and –0.215 a.u.), compared with the Ru(II) complex (–0.184 and –0.090 a.u., respectively). The d_π atomic orbitals (AO) of Ru(II) lie closer to π*-MO of cyano groups than the d_π-AO of Ir(III), which causes stronger effects of back electron density transfer for the $[Ru(bpy)_2(CN)_2]$ complex.

Table 1. Bond lengths (Å), bond angles, and dihedral angles (deg) for the ground state of $[Ru(bpy)_2(CN)_2]$ and $[Ir(bpy)_2(CN)_2]^+$ complexes

Parameter	Complex		
	$[Ru(bpy)_2(CN)_2]$		$[Ir(bpy)_2(CN)_2]^+$, calcd.
	found [16]	Calcd.	
$M–N_3$	2.051	2.076	2.067
$M–N_8$	2.108	2.124	2.121
$M–C_{14}$	1.991	2.022	1.991
$C_2–C_7$	1.481	1.474	1.478
$C_2–N_3$	1.365	1.379	1.378
$C_7–N_8$	1.350	1.376	1.374
$N_3–C_4$	1.334	1.366	1.361
$N_8–C_9$	1.335	1.359	1.356
$C_1–C_2$		1.409	1.405
$C_7–C_{12}$		1.410	1.406
$C_4–C_5$		1.400	1.401
$C_5–C_6$		1.409	1.406
$C_{14}–N_{15}$	1.146	1.193	1.187
$\angle MN_3C_4$	125.6	124.3	123.8
$\angle MN_8C_9$	126.7	125.7	125.7
$\angle MN_3C_2$	116.0	116.5	115.5
$\angle MN_8C_7$	114.9	115.1	114.3
$\angle N_3MC_{28}$	97.3	93.9	94.9
$\angle C_2C_7N_8C_9$		179.5	179.1
$\angle N_3C_2C_7N_8$	2.7	0.4	0.6

In the model of Dewar and Chatt–Duncanson [17, 18], the binding of the *d*-shell of the metal ion with the ligand is determined by the electron density transfer (donation) from the σ orbital of the CN group to the unoccupied *d*σ-AO of the metal ion and by the simultaneous back transfer from the occupied d_π-AO of the metal ion to the π*-antibonding MO of the cyano ligand. Indeed, the HOMOs of both complexes are mostly localized on CN groups, with a pronounced electron density transfer to the metal ion (Fig. 2a). The LUMO (Fig. 2b) has no

Table 2. Calculated frequencies ν (cm^{-1}), IR intensities IIR (km mol–1), and Raman intensities IRam ($Å^4$ a.m.u.$^{-1}$) for the ground state of the complexes under study

Mode	Type of vibrations[a]	$[Ru(bpy)_2(CN)_2]$			$[Ir(bpy)_2(CN)_2]^+$		
		ν	I_{IR}	I_{Ram}	ν	I_{IR}	I_{Ram}
113	ν(CN), in-phase	2066	61.7	257.7	2125	13.7	185.0
112	ν(CN), out-of-phase	2059	46.6	221.0	2117	14.7	124.5
111	ν(C=C), ν(C–C)	1603	3.7	145.9	1611	2.7	79.8
110	ν(C=C), ν(C–C)	1603	2.7	75.0	1610	11.1	65.3
109	ν(C=C), ν(C–C)	1598	0.01	462.9	1608	16.8	304.0
108	ν(C=C), ν(C–C)	1598	1.2	224.1	1607	24.6	252.9
107	ν(C=C), ν(C=N)	1563	6.0	13.9	1572	3.8	0.2
106	ν(C=C), ν(C=N)	1563	3.1	30.0	1572	1.1	2.4
105	ν(C=C), ν(C=N)	1550	0.1	179.0	1563	1.4	176.2
104	ν(C=C), ν(C=N)	1549	0.6	50.7	1563	5.9	104.7
103	ν(C–C), in-phase	1483	4.4	350.0	1498	1.5	225.1
102	ν(C–C), out-of-phase	1479	62.3	122.9	1497	1.4	98.4
101	δ(CH) + ν(C=N)chelate	1463	36.9	13.7	1470	36.6	4.3
100	δ(CH) + ν(C=N)chelate	1460	113.2	1.1	1467	120.3	0.6
99	δ(CH) + ν(C=N)chelate	1436	5.9	21.8	1445	20.0	0.7
98	δ(CH) + ν(C=N)chelate	1435	5.6	14.3	1444	31.5	0.5
97	δ(CH) + ν(C–C)	1423	68.1	5.9	1430	38.6	9.7
96	δ(CH) + ν(C–C)	1422	11.9	16.1	1429	9.0	13.2
95	ν(C=N)chelate + δ(CH)	1321	0.8	163.9	1330	8.5	0.8
94	ν(C=N)chelate + δ(CH)	1321	2.1	86.2	1329	3.5	4.2
93	ν(C–C) + δ (CH)	1321	4.1	24.9	1325	5.2	100.8
92	ν(C–C) + δ(CH)	1320	2.1	298.4	1324	0.3	317.3
91	ν(C=N) + ν(C=C) + δ(∠NMN)	1291	23.0	44.1	1300	0.4	44.5
90	ν(C=N) + ν(C=C) + δ(∠NMN)	1289	4.7	68.8	1299	0.2	51.0
89	ν(C=N) + ν(C=C) + δ(CH)	1277	3.1	76.6	1285	0.1	49.3
88	ν(C=N) + ν(C=C) + δ(CH)	1275	26.3	51.4	1283	5.2	24.5
87	ν(C=N) + ν(C=C) + δ(CH)	1273	4.8	126.2	1279	9.6	25.9
86	ν(C=N) + ν(C=C) + δ(CH)	1272	9.7	30.6	1279	11.9	14.1
85	δ(CH)	1182	0.1	50.9	1193	0.7	13.8
84	δ(CH)	1182	0.1	18.4	1193	4.5	4.1
83	δ(CH)	1173	3.7	1.1	1184	7.0	3.4
82	δ(CH)	1173	2.0	4.1	1184	3.0	10.5
79	δ(CH) + ν(ring)	1101	0.1	9.4	1110	1.4	32.4

Table 2. (Contd.)

Mode	Type of vibrations	$[Ru(bpy)_2(CN)_2]$			$[Ir(bpy)_2(CN)_2]^+$		
		ν	I_{IR}	I_{Ram}	ν	I_{IR}	I_{Ram}
78	δ(CH) + ν(ring)	1100	0.1	3.8	1109	8.7	6.5
75	δ(CH) + ν(ring)	1052	5.6	12.9	1060	4.7	4.3
74	δ(CH) + ν(ring)	1052	1.3	73.6	1059	0.9	31.2
73	δ(ring) + ν(M-N)	1036	1.7	2.6	1043	2.1	9.2
72	δ(ring) + ν(M-N)	1034	2.6	0.7	1043	2.2	7.5
69	Ring pulsation	1011	3.9	361.0	1030	0.02	237.1
68	γ(CH)	1001	0.7	1.93	1028	0.2	3.5
67	γ(CH)	1001	1.5	29.2	1028	0.1	0.6
66	Ring pulsation	997	61.1	153.3	1022	2.4	87.1
63	Ring pulsation	988	2.1	212.3	1007	4.4	36.3
62	Ring pulsation	984	13.7	100.7	1004	3.0	30.1
53	γ(CH)	777	160.3	1.0	789	154.1	0.1
52	γ(CH)	776	124.1	0.5	788	127.7	0.04
51	Ring pulsation	761	0.2	58.2	761	0.2	42.8
50	Ring pulsation	760	5.8	20.6	761	0.2	12.1
47	γ(CH)	748	18.8	1.5	749	12.1	2.3
46	γ(CH)	747	12.1	2.8	748	10.4	0.9
35	ω(MC) + ring torsion	484	4.9	0.7	489	1.6	0.4
34	τ(MC) + ring torsion	473	0.0	9.1	481	0.2	1.9
33	*r*(MC) + γ(ring) [in (II) δ(*b* ∠CIrC)]	467	2.7	7.4	470	0.04	7.8
32	δ(*b* ∠CIrC) + γ(ring)	464	1.2	5.6	469	0.7	1.3
31	ν(M–C), in-phase + γ(ring)	454	0.5	13.3	460	0.9	3.2
30	ν(M–C), out-of-phase + γ(ring)	435	7.9	2.4	440	8.9	3.8
29	ω(MC) + γ(ring) [in (II) *r*(IrC)]	431	6.3	1.1	438	2.8	2.4
28	τ(MC) + γ(ring)	430	5.4	0.7	432	5.9	2.1
27	τ(MC) + [in (II) ν(Ir–C) out-of-phase]	411	0.1	9.2	431	2.7	0.1
26	ν(M–C), out-of-phase + [in (II) δ(*b* ∠CIrC)]	403	1.5	7.1	427	2.9	6.1
25	δ(*b* ∠CMC) + γ(ring) [in (II) τ(Ir–C)]	383	7.8	3.2	421	3.2	5.8
24	*r*(MC) + γ(ring)	376	9.3	0.9	387	2.0	0.1
23	ν(M–C), in-phase	360	0.1	17.7	367	0.3	10.7
22	ν(M–N), out-of-phase	359	5.3	8.9	364	0.8	6.6

[a] ν, stretching vibration (bond stretching); deformation vibrations: δ(*b* ∠) scissor, ω fan-like, *r* pendular, τ torsion, and γ out-of-plane.

contribution from CN groups, it is mostly localized on bpy ligands and has a π*-antibonding nature in the pyridine rings. At the same time, this π*-MO is a bonding orbital with respect to the interring C–C bonds.

Analysis of vibration spectra of the $[Ru(bpy)_2(CN)_2]$ and $[Ir(bpy)_2(CN)_2]^+$ complexes. The vibration spectra of the molecules under study, which are composed of 45 atoms, have 129 normal vibrations. The most interesting

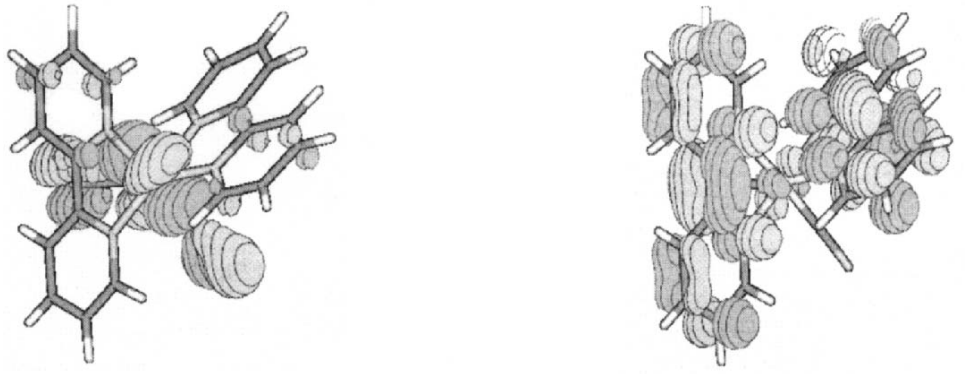

Fig. 2. (a) Highest occupied and (b) lowest unoccupied molecular orbitals of the $[Ru(bpy)_2(CN)_2]$ complex, calculated by the DFT/B3LYP method in the Lan12DZ basis.

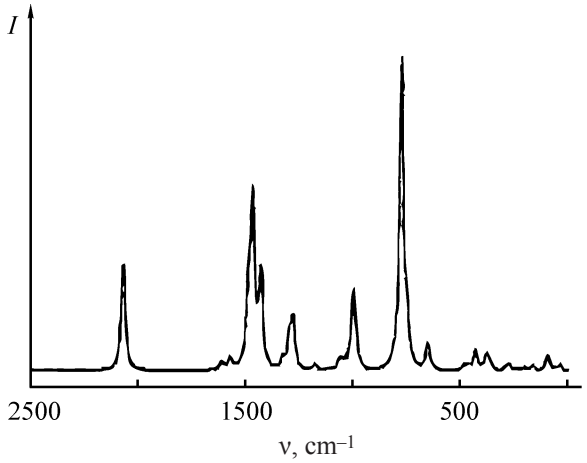

Fig. 3. IR spectrum of the [Ru(bpy)2(CN)2] complex in the S_0 state, calculated by the DFT/B3LYP method. Line half-width 10 cm^{-1}, I_{max} = 290.5 km mol^{-1}. (*I*) Intensity and (ν) wave number; the same for Figs. 4–6.

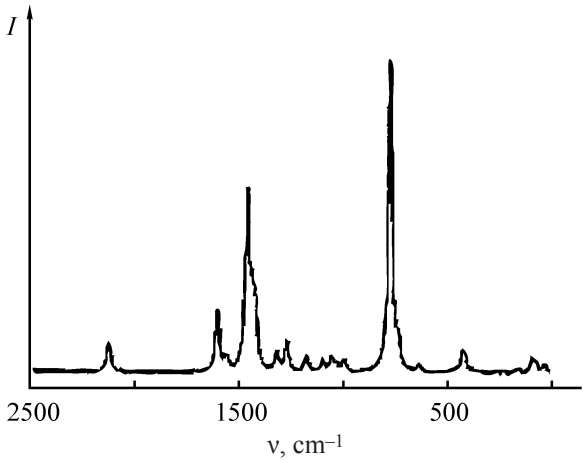

Fig. 4. IR spectrum of the $[Ir(bpy)_2(CN)_2]$+ complex in the S_0 state, calculated by the DFT/B3LYP method. Line half-width 10 cm^{-1}, I_{max} = 283.3 km mol^{-1}.

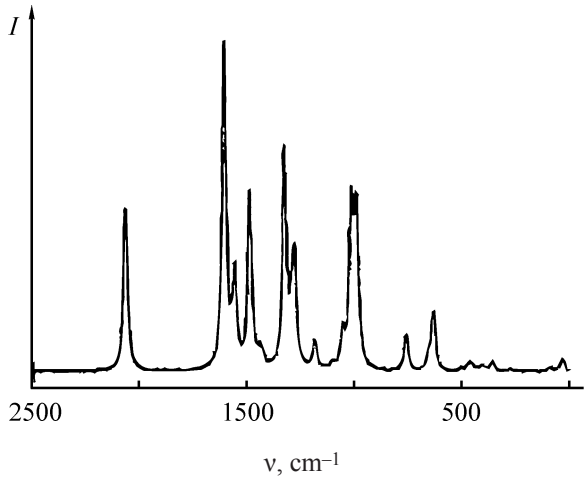

Fig. 5. Raman spectrum of the $[Ru(bpy)_2(CN)_2]$ complex in the S_0 state, calculated by the DFT/B3LYP method. Line half-width 10 cm^{-1}, I_{max} = 1310.8 $Å^4$ a.m.u.$^{-1}$.

of these, for analysis of the relationship between the structure and the spectra, are represented in Table 2, which lists the calculated forms of normal vibrations and their frequencies and intensities. In the table, a continuous numbering of all the normal modes is given in accordance with increasing vibration frequencies. Standard letter designations are used for assignment of vibration types.

Stretching vibrations of CN groups. According to Bellamy [15], the range 2200–2000 cm^{-1} is a characteristic range both for organic nitriles and for various inorganic compounds containing a –C≡N group. In the IR absorption spectrum of the compound *cis*-$[(4,4'-(CO_2H)_2bpy)_2Ru(CN)_2]$, the characteristic bands of a co-ordinated cyanide group are observed at 2073 and 2059 cm^{-1} [19]. In our calculation, the stretching vibrations of two CN groups at 2066 cm^{-1} (in-phase) and 2059 cm^{-1} (out-of-phase) in the IR spectrum of complex

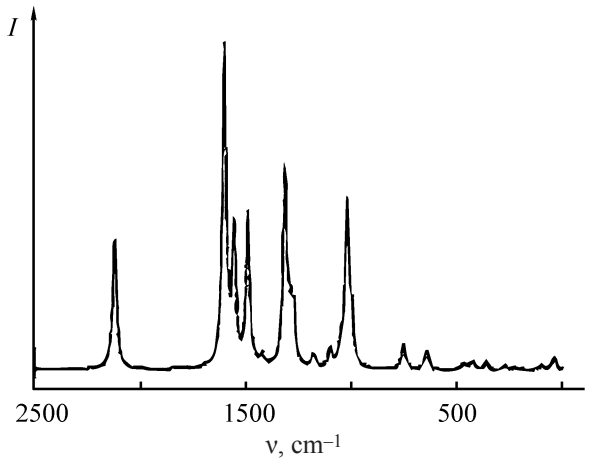

Fig. 6. Raman spectrum of the $[Ir(bpy)_2(CN)_2]^+$ complex in the S_0 state, calculated by the DFT/B3LYP method. Line half-width 10 cm^{-1}, I_{max} = 703.8 $Å^4$ a.m.u.$^{-1}$.

(I) form a medium-intensity absorption band (Fig. 3, Table 2). In the IR spectrum of complex (II), this band is shifted to higher frequencies (by approximately 60 cm^{-1}) (Fig. 4) and its intensity decreases (Table 2). In the Raman spectra of the complexes under study, the band of stretching vibrations of CN groups has a medium intensity (Table 2, Figs. 5 and 6). The considerable differences in the frequencies and intensities of vibrational modes of the stretching vibrations of the C≡N bonds in complexes (I) and (II) are due to differences in their force constants *k*, C≡N bond lengths, and bond polarities, which result from the nature of a complexing agent, Ru(II) or Ir(III). For example, *k*(C≡N) for complex (I) is 33.8 mdyne $Å^{-1}$ at a bond length of 1.193 Å, and that for complex (II), 35.6 mdyne $Å^{-1}$ at a bond length of 1.187 Å (Table 1). The C≡N bond is more polar in the complex $[Ir(bpy)_2(CN)_2]^+$, whereas the polarity of the M–C bond is higher in the complex with Ru(II) (Table 3).

C=C vibrations. Stretching vibrations of C=C bonds, with a minor contribution from stretching vibrations of C–C σ-bonds between the pyridine rings, are manifested in a narrow frequency range (modes 111–108, Table 2). In the IR spectrum of complex (I), to these vibrations corresponds a very weak band peaked at 1603 cm^{-1} (*I* = 3.7 km mol^{-1}). In the IR spectrum of complex (II), this band is shifted by only 4 cm^{-1} to higher frequencies, but is more intense (*I* = 24.6 km mol^{-1}). In the Raman spectrum, this type of vibrations gives rise to the most intense band peaked at 1598 cm^{-1} for complex (I) (Fig. 4), and at 1608 cm^{-1} for complex (II) (Fig. 6). There are no published experimental data for the IR and Raman spectra of the complexes, calculated in this study, and, therefore,

Table 3. Charges on atoms and ligands, calculated by Mulliken for the ground state of the $[Ru(bpy)_2(CN)_2]$ and $[Ir(bpy)_2(CN)_2]^+$ complexes

Atom or ligand	Charge in elementary charge units	
	$[Ru(bpy)_2(CN)_2]$	$[Ir(bpy)_2(CN)_2]^+$
M	0.726	0.690
C^{14}	–0.253	–0.244
N^{15}	–0.228	–0.132
bpy	0.118	0.531
CN	–0.481	–0.376

we used, for comparison, spectra of similar bipyridyl complexes, reported in [14, 19–23]. The comparison yielded rather close results. For example, in the SERRS spectrum of the $[Fe(bpy)_2(CN)_2]$ complex, the band of stretching vibrations ν(C=C) is observed at 1604 and 1607 cm^{-1} for the $[Ru(bpy)_3]^{2+}$ complex [14]. The Raman spectrum of the $[Ni(bpy)(H_2O)_2]SO_4$ complex contains an intense band at 1604 cm^{-1} (in aqueous solution) and 1603 cm^{-1} (in a solid sample) [20]. The close values of the calculated and experimental frequencies of different complexes confirm the above conclusion that the structure of bipyridyl ligands only slightly depends on the nature of a metal ion.

C=C and C=N vibrations. The interaction of vibrations of aromatic C=C and C=N bonds of pyridine rings gives rise to a very weak absorption band peaked at 1563 cm^{-1} in the IR spectra of the Ru(II) and Ir(III) complexes under study (Table 2, modes 107–104; Figs. 3, 4). In the Raman spectrum, the bands corresponding to these ring vibrations, peaked at 1550 cm^{-1} for complex (I) and 1563 cm^{-1} for complex (II), have medium intensities (Figs. 5, 6). Comparison with the known experimental data for similar metal-complexes of bypyridyls again gives a good agreement.

In [14], the band at 1564 cm^{-1} in the resonance Raman spectrum of the $[Fe(bpy)_2(CN)_2]$ complex and the band at 1562 cm^{-1} for $[Ru(bpy)_3]^{2+}$ were assigned to ν(C=C) vibrations, which not quite corresponds to the calculated animation of vibrations. In free 2,2'-bipyridine, ν(C=C) and ν(C=N) vibrations are mixed, according to the results of our calculations, with ν(C=C) and ν(C–C) vibrations and give rise to a medium-intensity band in the IR spectrum, peaked at 1580 cm^{-1}, and the most intense band at 1586 cm^{-1} in the Raman spectrum of 2,2'-bipyridine. These vibrations are similar to those experimentally found

in the Raman spectrum of a free ligand at 1579 cm^{-1} for a single crystal (1591 cm^{-1} in a CCl_4 solution) [21]. In the IR spectrum of the solution, they are observed at 1579 cm^{-1} [22], also in good agreement with our calculation for 2,2'-bipyridine. The shift of these frequencies in the ligand upon complexation (Table 2) is undoubtedly due to bipyridine flattening and to enhanced conjugation between the rings.

Vibrations of the interring C–C σ-bond. Due attention has not been given in the literature to analysis of vibrations of the interring C–C σ-bond. However, our calculations demonstrated that these vibrations are of fundamental importance for vibronic interactions and related effects in electronic spectra. Bands of stretching vibrations of C–C bonds in the sensitizing dyes under study are intense in Raman spectra, especially in the excited triplet (T1) state if the complex becomes asymmetric upon excitation. As can be seen in Table 2, vibrations of the C–C σ-bond are responsible for vibrational modes 103 and 102, which form a narrow medium-intensity band in the Raman spectrum, peaked at 1483 cm^{-1} for complex (I) (Fig. 5) and at 1498 cm^{-1} for complex (II) (Fig. 6), and also for modes 97, 96 (1423 cm^{-1}) and 95–92, which form a very intense band at 1320 cm^{-1} for complex (I) [1324 cm^{-1} for complex (II)] (Figs. 5, 6). In modes 97–92, vibrations of C–C bonds are mixed with planar deformation vibrations of CH. In [14], the bands at 1489 and 1430 cm^{-1} in the SERRS spectrum of the $[Fe(bpy)_2(CH)_2]$ complex were assigned to mixed ν(C=N) and δ(CH) vibrations; in [12], the band at 1488 cm^{-1} for the $[Ru(bpy)_2(BIK)]^{2+}$ complex was attributed to ν(C=C) vibrations mixed with δ(CH).

According to quantum-chemical calculations, mixed δ(CH) and ν(C=N) vibrations of chelate cycles at frequencies in the range 1460–1470 cm^{-1} (modes 101 and 100), as well as ν(C=C) and ν(C=N) vibrations of pyridine rings, mixed with planar deformation vibrations of CH at 1445–1435 cm^{-1} (modes 99, 98), do occur, but are low-active in Raman spectra. Therefore, band assignments in [12, 14] are not quite correct. A DFT B3LYP calculation yields a more accurate interpretation of Raman bands in this spectral range.

The intense band peaked at 1320 cm^{-1} in the Raman spectrum of complex (I) (Fig. 5) has an additional peak at 1273 cm^{-1}, resulting from combination of asymmetric bond vibrations in pyridine rings and deformation vibrations of CH (modes 91–86). These vibrations are less active in complex (II) and do not lead band splitting, with only steps formed on the right wing of the band at 1324 cm^{-1}, associated with vibrations of the C–C σ-bond (Fig. 6). Vibrations of the C–C σ-bond, with a pronounced contribution from δ(CH) vibrations, have been observed at 1317 cm^{-1} in the SERRS spectrum of the $[Ru(bpy)_2(BIK)]^{2+}$ complex and at 1321 cm^{-1} in the spectrum of the $[Fe(bpy)_2(CN)_2]$ complex [14]. The band at 1274 cm^{-1} was not assigned in [12].

Specific features of the IR spectra in this spectral range should be noted. In the IR spectrum of complex (I), the absorption associated with out-of-phase ν(C–C) vibrations (1479 cm^{-1}, Fig. 3), which corresponds to vibrational mode 102 (Table 2) and has a medium intensity (62.3 km mol^{-1}), overlaps with a more intense band associated with deformation vibrations of CH and ν(C=N) of chelate rings, peaked at 1460 cm^{-1} (I = 113.2 km mol^{-1}). An additional peak at 1423 cm^{-1} on the right wing of this band is due to deformation vibrations δ(CH) mixed with stretching vibrations of the C–C σ-bond (modes 97, 96). In the IR spectrum of complex (II), these mode are less intense and, together with modes 99, 98 (ν_{calc} 1445 and 1444 cm^{-1}), form only a shoulder on the main band of deformation vibrations of CH groups (modes 101 and 100, Fig. 4).

ν(C–C) and δ(CH) vibrations at 1321 cm^{-1} (modes 95–92) in the IR spectrum of complex (I) form only a weak shoulder on the weak absorption band associated with ring vibrations and deformation vibrations of CH (modes 91–86, Fig. 3). In the case of complex (II), modes 95–92 and 91–86 form separate weak, but clearly pronounced peaks at 1330 and 1279 cm^{-1} (Fig. 4). In [23], the variable-intensity absorption band at 1308–1313 cm^{-1} in IR spectra of transition metal complexes of composition $[M(bpy)Cl_2]$ was assigned to ring vibrations and deformation vibrations of CH, which coincides with the assignment made in the present study. The weak band at 1280–1265 cm^{-1} was assigned in [23] to vibrations of the ring and of the C–C interring bond. Calculation gives a somewhat different nature for this band: there is no contribution from the C–C bond in these modes (91–86), although ring vibrations are present.

Deformation vibrations of CH and ring vibrations. In the calculated IR spectrum of a free 2,2'-bipyridyl ligand, planar deformation vibrations of CH give rise, without admixture of other vibrations, to an exceedingly weak narrow band at 1170 cm^{-1}. In complex (I), these vibrations occur at 1182–1173 cm^{-1} (modes 85–82), being shifted in complex (II) by 11 cm^{-1} to higher frequencies (Figs. 3, 4). In the range 1130–1050 cm^{-1}, δ(CH) vibra-

tions are mixed with skeletal stretching vibrations of the ring and form weak bands in IR and Raman spectra of the Ir(III) complex and a shoulder at 1052 cm^{-1} on the left wing of a stronger band associated with pulsation vibrations of pyridine rings.

Out-of-plane vibrations of CH appear at the following frequencies (cm^{-1}): in complex (I), at 1020 (modes 71, 70), 1001 (modes 68, 67), 993 (modes 65, 64), 979–776 (modes 61–52), 756, and 563–502 (modes 39–36); in complex (II), at 1032, 1028, 1008, 991–778, 749 (modes 49, 48), and 559–494 cm^{-1}, respectively. γ(CH) vibrations form the most intense band at 777 cm^{-1} in the IR spectrum of the ruthenium complex and at 789 cm^{-1} in the IR spectrum of the iridium complex (Figs. 3, 4). The corresponding intense absorption band in the IR spectrum of the $[Pd(bpy)Cl_2]$ complex is observed at 780 cm^{-1} [23]. This type of vibrations does not show any activity sufficient for independent bands to be formed in Raman spectra of the complexes under study (Table 2).

Strong planar deformations of pyridine rings occur near 1034 cm^{-1} for complex (I) (modes 73, 72) and 1043 cm^{-1} for complex (II), but they are low-active in the IR and Raman spectra of these complexes.

Vibrational modes 69, 66, 63, 62, 51, and 50 are due to pulsation vibrations (breathing) of the rings. Strong differences between the frequencies of such vibrational modes (Table 2, 19–25 cm^{-1}) should be noted when comparing the vibrational spectra of the Ru(II) and Ir(III) complexes. To ring pulsations in the Raman spectrum of complex (I) corresponds a strong doublet band peaked at 1011 and 988 cm^{-1} and a weak band at 761 cm^{-1}. In complex (II), ring pulsations give rise to an intense band peaked at 1030 cm^{-1}, in whose formation modes 69–62 are superimposed, and a weak band at 761 cm^{-1}. A doublet band peaked at 1041 and 1029 cm^{-1} has been assigned to ring pulsations in a SERRS spectrum of the $[Ru(bpy)_2(phen)]^{2+}$ complex [12]; similar bands (at 1034 and 1024 cm^{-1}) have been observed for the $[Fe(bpy)_2(CN)_2]$ complex [14]. The superposition of modes 69–60 in the frequency range 1011–978 cm^{-1} gives rise to an absorption band with a lower-than-medium intensity in the IR spectrum of complex (I) (ν_{max} = 997 cm^{-1}). The main contribution to the intensity of this band (I = 61.1 km mol^{-1}) is made by vibrational mode 66, caused by ring pulsations. To ring pulsations in the IR spectrum of complex (I) corresponds a very weak band peaked at 1007 cm^{-1} (superposition of modes 66–62). Such bands were observed in [23] in IR spectra of the $[Pd(bpy)Cl_2]$, $[Pt(bpy)Cl_2]$, and $[Fe(bpy)Cl_2]$ complexes.

Vibrational modes 45–40 in the frequency range 670–630 cm^{-1} belong to planar deformation vibrations of the rings. In the range 490–473 cm^{-1} (modes 35, 34), there occurs planar torsion of the rings. In the IR spectrum of complex (I) these vibrations form weak bands peaked at 654 cm^{-1} (I = 17 km mol^{-1}) and 484 cm^{-1} (I = 4.9 km mol^{-1}). For complex (II), the intensity of IR absorption of these bands (ν_{max} 648 and 484 cm^{-1}) is even lower (2.6 and 1.6 km mol^{-1}, respectively). In [23], planar deformation vibrations of rings in the experimental IR spectrum of the $[Pd(bpy)Cl_2]$ complex were observed in the range 662–645 cm^{-1}. A medium intensity was only found for the absorption at 650 cm^{-1}. For the $[Pt(bpy)Cl_2]$ complex, a weak absorption is observed at 670–640 cm^{-1}. Very weak bands at 478 cm^{-1} for the palladium complex and at 482 cm^{-1} for the platinum complex in [23] were not assigned. We attribute these bands to modes 35, 34 and note that the ring torsion is mixed here with fan-type and pendular vibrations of metal–carbon bonds. This is highly important for the dynamics of electron transfer from an excited $[Ru(bpy)_2(CN)_2]$ molecule to the surface of titanium oxide.

In the Raman spectrum of complex (I), planar deformation vibrations of the rings form a band at 636 cm^{-1} with a lower-than-medium intensity (I = 100.7 $Å^4$ a.m.u.$^{-1}$; modes 35 and 34, having a contribution from the planar twisting of rings, combine with modes 33–31, having a contribution from out-of-plane deformation vibrations of the rings, and give rise to a broad weak band in the range 484–454 cm^{-1}. In [14], to planar deformation vibrations of the rings were attributed weak peaks at 659, 638, 494, and 479 cm^{-1} in the SERRS spectrum of the $Fe(bpy)_2(CH)_2]$ complex and at 667, 646, 554, and 401 cm^{-1} in that of the $[Ru(bpy)_3]^{2+}$ complex. This assignment is in agreement with the results of DFT calculations.

According to the results of our calculations, the out-of-plane deformation vibrations of the rings must occur in the ranges 467–430 and 403–376 cm^{-1} in the ruthenium complex and at 469–427 and 387 cm^{-1} in the iridium complex (Table 2). These vibrations are mixed with M–C vibrations to form very weak bands in the IR and Raman spectra. In the SERRS spectrum of $[Fe(bpy)_2(CN)_2]$, to out-of-plane vibrations of the rings are attributed weak peaks at 452 and 435 cm^{-1}; for the $[Ru(bpy)_3]^{2+}$ complex, these peaks are observed at 454 and 438 cm^{-1} [14]. At frequencies lower than 280 cm^{-1} occurs out-of-plane rocking of the rings. It is noteworthy that skeletal ring

vibrations in the range 1130–200 cm^{-1} lead to changes in the M–N bond lengths.

M–CN and M–N vibrations. These vibrations are the most important for induction of vibronic perturbations in electron shells of excited complexes. Vibrational modes 35–24 in the frequency range 490–370 cm^{-1} belong to metal–carbon stretching and deformation vibrations mixed with ring vibrations. In the IR spectrum of complex (I), to these vibrations correspond two weak bands at 435 cm^{-1} [out-of-phase ν(Ru–CN)] and 376 cm^{-1} (pendular vibrations of RuC). In the IR spectrum of complex (II), Ir–CN vibrations occur, according to our calculations, at higher (by 5–44 cm^{-1}) energies and a rearrangement of vibrational modes is observed (Table 2; modes 33, 29, 27, 26, and 25). In the given spectrum, all modes of Ir–C vibrations are superimposed to give only a single broad band peaked at 440 cm^{-1}, which is due, as in complex (I), to out-of-phase stretching vibrations ν(M–CN). The out-of-plane ring deformations involved in these vibrations cause deformation of interring C–C bonds, and, therefore, it is quite natural that the weak IR absorption by transition metal complexes of the type $[M(bpy)Cl_2]$ in the range 442–445 cm^{-1} was attributed in [23] to deformation vibrations of C–C.

In the Raman spectrum of complex (I), Ru–CN vibrations also form two weak bands peaked at 454 cm^{-1} [in-phase ν(Ru–CN)] and 411 cm^{-1} (torsion vibrations of RuC), and in that of complex (II), at 469 and 427 cm^{-1} (scissor vibrations of IrC fragments).

To stretching vibrations of M–N correspond vibrational modes 23 and 22, which give weak bands at 360 cm^{-1} in Raman spectra; ν(M–N) cause in-phase (mode 23) and out-of-phase (mode 24) pulsation vibrations of chelate rings.

In [14], to stretching vibrations ν(M–N) in the SERRS spectra corresponds band at 371 cm^{-1} for the $[Ru(bpy)_3]^{2+}$ complex and bands at 385 and 367 cm^{-1} for the $[Fe(bpy)_2(CN)_2]$ complex. The band at 385 cm^{-1} is associated with deformation vibrations of M–N and out-of-plane vibrations of the rings. Such a difference in the interpretation of a weak Raman band is of fundamental importance, because this mode is active under electronic excitation.

CONCLUSIONS

(1) A theoretical simulation by calculations using the density-functional method demonstrated a good agreement in all details with experimental spectra for related compounds of bipyridyl complexes with metal ions of the platinum group.

(2) The results of this study can serve as a reliable theoretical basis for classification of electronic and structural factors determining the frequencies and intensities of bands in IR and Raman spectra of metal-complexes of the $[M(bpy)_2(CN)_2]$ type.

(3) A comparison of the simulated spectra with their experimental analogs revealed a number of vibrations found to be sensitive to the nature of a metal. Especially important are predictions of the frequencies and IR intensities of metal ion vibrations, based on first-principles calculations.

(4) Simulation of IR and Raman spectra by DFT, combined with the available experimental information for a series of related complexes, can be used to explain the nature of previously incompletely assigned band. An empirical choice of the force field and a calculation of vibrations, performed 30 years ago, fail to provide a full understanding of all IR and Raman bands; this primarily refers to vibrations involving a metal ion.

ACKNOWLEDGMENTS

The study was carried out in the framework of the Romanian-Ukrainian program "Development of new sensitizing dyes for nanocrystalline TiO_2 for solar cells by calculation of their electronic structure" (project no. 11.571/31.01.2008) and Swedish-Ukrainian Visby program "Light-emitting diode materials" (project no. 01403/2007).

REFERENCES

1. Hagfeldt, A. and Gratzel, M., *Acc. Chem. Res*., 2000, vol. 33, no. 5, pp. 269–277.
2. Monat, J.E., Rodriguez, J.H., and McCusker, J.K., *J. Phys. Chem. A*, 2002, vol. 106, no. 32, pp. 7399–7406.
3. Minaev, B., Minaeva, V., and Vahtras, O., *Proc. NanoSol-Net Int. Symp.: Trends in Organic Electronics and Hybrid Photovoltaics*, Girtu, M.A. and Fahlman, M., Eds., Eforie Nord, Romania, June 12–14, 2008. Constanta, Ovidius Univ. Press, 2008, pp. 142–147.
4. Aiga, F. and Tada, T., *J. Mol. Struct*., 2003, vol. 658, no. 1, pp. 25–32.
5. Minaev, B., Minaeva, V., and Agren, H., *J. Phys. Chem. A*, 2009, vol.113, no. 4, pp. 726–735.

6. Baranovskii, V.I., Lyubimova, O.O., Makarov, A.A., and Sizova, O.V., *Zh. Strukt. Khim*., 2002, vol. 43, no. 3, pp. 407–417.
7. Mallick, P.K., Danzer, G.D., Strommen, D.P., and Kincaid, J.R., *J. Phys. Chem.,* 1988, vol. 92, no. 20, pp. 5628–5634.
8. Becke, A.D., *J. Chem. Phys*., 1993, vol. 98, no. 7, pp. 5648–5652.
9. Burke, K., Werschnik, J., and Gross, E.K.U., *J. Chem. Phys.*, 2005, vol. 123, no. 6, p. 062206.
10. Lee, C., Yang, W., and Parr, R.G., *Phys. Rev. B*, 1988, vol. 37, no. 2, pp. 785–789.
11. Frisch, M.J., Trucks, G.W., Schlegel, H.B., et al., *Gaussian 03, revision C.02,* Gaussian, Inc., Wallingford, CT, 2004.
12. Jang, Y.M., Nam, S., Lim, J.W., et al*., Bull. Korean Chem. Soc.*, 1998, vol. 19, no. 3, pp. 372–375.
13. Jang, Y.M., Lim, J.W., Kim, E.R., et al., *Bull. Korean Chem. Soc.*, 2001, vol. 22, no. 3, pp. 318–320.
14. Dines, T.J. and Peacock, R.D., *J. Chem. Soc. Faraday Trans. 1*, 1988, vol. 84, no. 10, pp. 3445–3457.
15. Bellamy, L.J., *The Infrared Spectra of Complex Molecules*, London: Chapman & Hall, 1975, vol. 1.
16. Guillemoles, J.-F., Barone, V., Joubert, L., and Adamo, C., *J. Phys. Chem. A,* 2002, vol. 106, no. 46, pp. 11354–11360.
17. Dewar, M.J.S., *Bull. Societe Chim. France,* 1951, vol. 18, nos. 3–4, pp. 71–79.
18. Chatt, J. and Duncanson, L.A.*, J. Chem. Soc.*, 1953, p. 2939.
19. Heimer, T.A., Bignozzi, C.A., and Meyer, G.J., *J. Phys. Chem.,* 1993, vol. 97, no. 46, pp. 11987–11994.
20. Muniz-Miranda, M., *J. Raman Spectrosc*., 2000, vol. 31, no. 7, pp. 637–639.
21. Castellucci, E., Angeloni, L., Neto, N., and Sbrana, G., *Chem. Phys.*, 1979, vol. 43, no. 3, pp. 365–373.
22. Strukl, J.S. and Walter, J.L., *Spectrochim. Acta,* 1971, vol. 27A, no. 2, pp. 209–221.
23. Strukl, J.S. and Walter, J.L., *Spectrochim. Acta,* 1971, vol. 27A, no. 2, pp. 223–238.